IOSR Journal of Engineering (IOSRJEN)
ISSN: 2250-3021 ISBN: 2878-8719 PP 37-43
National Symposium on engineering and Research

Study of Failure Analysis of Gas Turbine Blade

Patil A.A.*, Shirsat U.M.
Department of Mechanical Engineering, SND COE & RC Yeola, Nashik, India

Abstract: *- The failure of a second stage blade in a gas turbine was investigated by metallurgical and mechanical examinations of the failed blade. The blade was made of a nickel-base alloy Inconel 738LC. The turbine engine has been in service for about 73,500 hrs. Before the blade failure. Due to the blade failure, the turbine engine was damaged severely. The investigation was started with a thorough visual inspection of the turbine and the blades surfaces, followed by the fractography of the fracture surfaces, micro structural investigations, chemical analysis and hardness measurement. The observation showed that a serious pitting was occurred on the blade surfaces and there were evidences of fatigue marks in the fracture surface. The micro structural changes were not critical changes due to blade operation at high temperature. It was found that the crack initiated by the hot corrosion from the leading edge and propagated by fatigue and finally, as a result of the reduction in cross-section area, fracture was completed. An analytical calculation parallel to the finite element method was utilized to determine the static stresses due to huge centrifugal force. The dynamic characteristics of the turbine blade were evaluated by the finite element mode and harmonic analysis. Finally according to the log sheet records and by using a Campbell diagram there was a good agreement between the failure signs and FEM results which showed the broken blade has been resonated by the third vibration mode occasionally before the failure occurred.*
Keywords: *- Blade failure; hot corrosion; Fatigue failure; Inconel 738LC; Finite element*

1. Introduction

1.1 Gas Turbine Working Principle

A schematic drawing of a simple gas turbine is shown in figure 1.1. The working principle behind the gas turbine is as follows. Ambient air is compressed in the compressor. This compressed air is directed to the combustion chamber. In the combustion chamber the compressed air is mixed with vaporized fuel and burned under constant pressure. This burning process results in a hot gas with high energy content. This hot gas is allowed to expand through the turbine where the energy in the gas is converted to a rotation of the turbine shaft. The turbine shaft powers both the compressor and a generator used to obtain electrical power from the gas turbine.

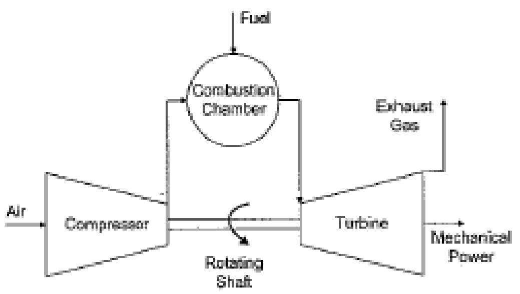

Fig.1.1: A simple gas turbine.

1.2 Turbine Blade

Super alloys were developed since the second quarter of the 20th century as materials for elevated temperature applications and can be divided in three groups: nickel-base super alloys, cobalt-base super alloys and iron base super alloys. Gas turbine blades are principally made of nickel-base and cobalt-base super alloys. The main reason for the existence of super alloys is their outstanding strength at elevated temperatures, which make them suitable for the fabrication of gas turbine components. During the operation of power generation gas turbines, the blades and other elements of hot gas path undergo service-induced degradation, which may be natural or accelerated due to different causes.

The degradation or damage may have a metallurgical or mechanical origin and results in reduction of equipment reliability and availability. To identify the causes of the blade failures, a complete investigation has to be carried out, integrating both the mechanical analyses and metallurgical examination. Metallurgical examination can be very effective in determining whether the failure is related to material defects, mechanical marks, poor surface finish, initial flaws or heat treatment.

There are different factors, which influence blade lifetime, as design and operation conditions but the latter are more critical. In general, most blades have severe operation conditions characterized by the following factors

1) Operation environment (high temperature, fuel and air contamination, solid particles, etc.).
2) High mechanical stresses (due to centrifugal force, vibratory and flexural stresses, etc.).
3) High thermal stresses (due to thermal gradients).

Typically there are acting two or more factors simultaneously causing reduction of blade lifetime. The type of damage, which occurs in gas turbine blades and nozzles after a service period, can be divided into

1)External and internal surface damages (corrosion, oxidation, crack formation, erosion, foreign object damage and fretting).

2)Internal damage of microstructure, such as c0[Ni3(Al,Ti)] phase aging (rafting), grain growth, creep and grain boundary void formation, carbides precipitation and brittle phases formation.Surface damage produces blades/nozzles dimensional changes, which result in operational stress increase and turbine efficiency deterioration.In service, blade material deterioration is related to the high gas temperature, high steady state load levels (centrifugal load) and high thermal transient loads (trips, start-ups and slowing downs). However, the degree of deterioration in individual blades differs due to several factors such as:

1) Total service time and operation history (number of start-ups, shut-downs and trips).

2)Engine operational conditions (temperature, rotational speed, mode of operation (base load, cyclic duty)).

3)Manufacturing differences (grain size, porosity, alloy composition, heat treatment).

The Inconel 738LC alloy commonly used for gas turbine blades is strengthened by precipitation of c0 phase. The micro structural changes due to blade operation at high temperature include irregular growing of particles (rafting) and formation of carbides in grain boundaries and matrix. This leads to alloy creep properties reduction.

In order to have an instrument for the deterioration evaluation of gas turbine blade alloy, it is necessary to associate the influence of service-induced micro structural degradation to the changes in mechanical properties. This can be used for monitoring and evaluation of extent and degree of material damage and lifetime consumed and to obtain recommendations for blade rejuvenation treatments, operation and reposition.

Application of effective methods of material deterioration evaluation can be used for practical lifetime prediction, just in-time blade rehabilitation (rejuvenation), safe and cost-effective lifetime extension and to avoid blade catastrophic failure. In the other hand most of gas turbo generators are used as an auxiliary compensator in power plants to generate electric power at the peak of load demand. Thus they often are utilized in discontinuous conditions of commissioning. This subject leads them to a lot of shocks and risks. Therefore it seems the failure analysis is a good manner for detecting the root causes. So according to the results of failure analysis, the gas turbine would be utilized by applying some new policies in the protected conditions. Often by using an intelligent mechanical analysis, the root causes of a failure could be revealed. Recently the computer programs and software packages are generalized to calculate the mechanical behavior of gas turbine blades. In this paper the ANSYS code was applied for generating and simulating a FE model of fractured blade. Previously there were many studies on the performance analysis of Gas turbine blade.

E. Poursaeidi, M. Aieneravaie (1) an analytical calculation parallel to the finite element method was utilized to determine the static stresses due to huge centrifugal force. The dynamic characteristics of the turbine blade were evaluated by the finite element modal and harmonic analyses. Finally according to the log sheet records and by using a Campbell diagram there was a good agreement between the failure signs and FEM results which showed the broken blade has been resonated by the third vibration mode occasionally before the failure occurred.

A. Kermanpur (2) the failure mechanism of Ti6Al4V compressor blades of an industrial gas turbine was analyzed by means of both experimental characterizations and numerical simulation techniques. Several premature failures were occurred in the high pressure section of the compressor due to the fracture of the blade roots. Metallurgical and mechanical properties of the blade alloy were evaluated. A 2D finite element model of the blade root was constructed and used to provide accurate estimates of stress field in the dovetail blade root and to determine the crack initiation in the dovetail. The results showed no metallurgical and mechanical deviations for the blade materials from standards. It was concluded that this failure has occurred due to the tight contact between the blade root and the disk in the dovetail region as well as low wear resistance of the blade root.

Z. Mazur(3) The failure analysis of the 70 MW gas turbine first stage blade made of nickel base alloy inconal 738LC is presented. The blade experience internal cooling hole crack in different aerofoil section assisted by a coating and base alloy degradation due to operation at high temperature. the detailed analysis of all the element which had an influence on the failure initiation was carried out , namely loss of aluminum form coating due to oxidation and coating phase changing decreasing of alloy ductility and toughness due to carbide precipitin in grain boundaries degradation of alloy gamma prime phase, blade aerofoil stress level evidence of intergranular creep crack propagation. It was found that the coating crack initiation and propagation was driven by a mixed fatigue mechanism.

Jung-Chel Chang (4) the failure of a gas turbine first stage bucket was investigated by visual inspection and finite element analysis. The failure of major bucket cooling passage was a critical cause of the separation of a bucket segment and cause microstructure deterioration of the neighboring region by serious thermal load. Change of microstructure morphologies of the damaged bucket under the thermal and mechanical stress was observed. After coating stripping. The bucket surface condition was evaluated through visual inspection and finite element analysis. The thermal mechanical fatigue cracking of surface coating.

2. ANALYSIS OF TURBINE BLADE

This includes the analysis of gas turbine blade. Analysis contains the visual examination, chemical analysis, hardness measurement, metallographic examination and analysis of fracture surfaces.

2.1 Experimental Procedure

The blade material was a cast Ni-base super alloy known as Inconel 738LC with the mechanical specifications that is presented in Table 1. Because of relation between the working temperature of alloys and their specifications, the tensile yield strength of all parts at the working temperatures were considered along this case study. According to the thermal conditions at the peak load of these types of gas turbine engine, the temperature of combustion products around the surfaces of airfoil arises up to 560 °C on the leading edge and 520 °C on the trailing edge (Fig.2.1).

The turbine has been in service for about 73,500 h and due to the blade failure the turbine engine was damaged severely. In addition to the failed blade, two adjacent blades were subjected to the laboratory for extensive failure analysis. The following sequence of examination was performed on the blades:

1. Visual examination and photographic documentation.
2. Hardness measurement of the transverse section beneath the fracture surface.
3. Chemical analysis of the blade material.
4. Metallographic examination of the transverse section of samples from the airfoil and root blade, and microprobe analysis.
5. Examination of the fracture surface by means of optical and electron microscopes.

Table 1
Material properties of alloys at the ambient temperature [10–12]

Component	Material	Mass density (kg/m^3)	Tensile yield strength [Min] (Pa)	Tensile ultimate strength (Pa)
Bucket	IN-738LC	8110.0	9.5×10^8	1.1×10^9
Disc	A471-Cl.10	7800.0	6.2×10^8	7.25×10^8

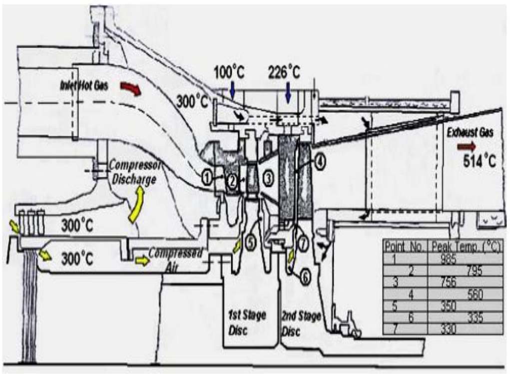

Fig. 2.1 The sketch view of turbine's hot section with temperatures of some important points

3.2 Visual Examination

Fig. 2 .2a and b shows the failed blade in the second stage of turbine, which signed as number 1. As a result of failure the fragmented part has damaged the leading edges and shroud tips of some blades (Fig. 2.2b). Three blades were submitted to the laboratory. The tip regions of the blades 2 and 3 were severely damaged presumably by impact; however the tip damage was not the focus of this investigation. All three blades were corroded by the pitting mechanism. The region of pitting on the concave surface of the airfoil was near the leading edge, and on the convex surface was near the trailing edge (Figs. 2.3 a and b). The pits on the leading edge were more critical and in some cases appeared like the transverse notches (Fig. 2.4). It should be noted that the height of the fracture surface from the platform at leading edge in blade number 1 was the same as the position of critical pits in blade number 3 (Fig. 2.5). There was not a considerable deposit on the blades surfaces.

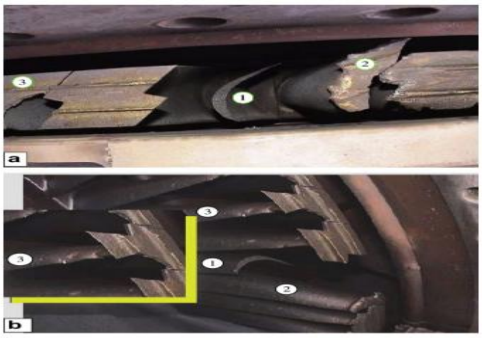

Fig.2.2. Position of the failed blade and the damages were caused due to failure.
(a) Upper view of the failed blade and surroundings.
(b) Leading edge damage in some blades.

Fig. 2.3 General view of the blade number 3 showing corroded regions.
(a) Concave surface. (b) Convex surface.

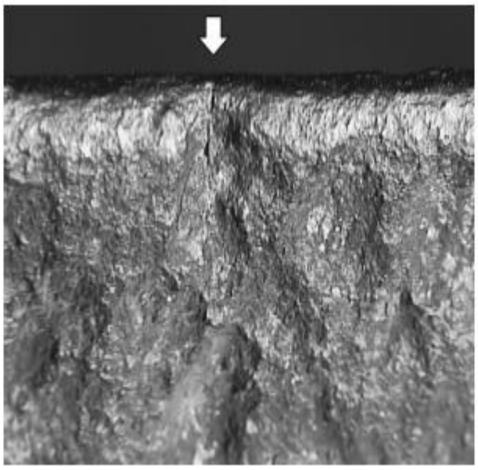

Fig. 2.4. The critical pit which is encircled in Fig. 2.3a. 20x.

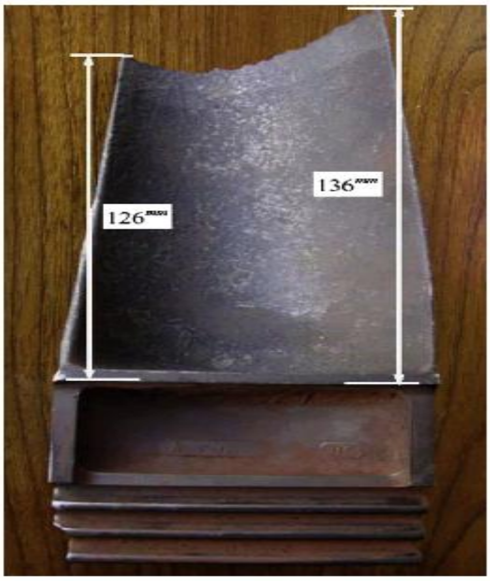

Fig. 2.5. The distance of the fracture surface from the platform at blade edges.

2.3 Chemical Analysis

To determine the chemical composition of the blade material a bulk analysis was performed by an Optical Emission Analyzer, ARC-MET 930 S&P. The result of chemical analysis showing that the material is in accordance with Inconel 738LC (Table 2).

2.4 Hardness Measurement

The hardness of the transverse section of the blade beneath the fracture surface was measured by a Universal Hardness Measurement Machine, SWISS MAX 300. Fig. 2.6 shows the points of hardness measurement on the blade cross-section. The results are given in Table 3. It is observed that there was no substantial change in the material's hardness, and thermal effects did not influence the strength of the material.

Table 2
Chemical composition of Inconel 738LC superalloy (wt%)

Alloy	Ni	C	Cr	Co	Mo	W	Al	Ti	B
IN 738LC	Bal	0.11	16	8.5	1.75	2.6	3.4	3.4	0.01

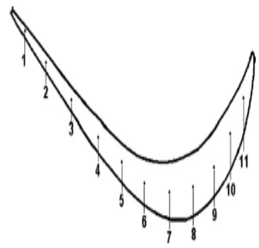

Fig. 2.6. Points of hardness measurement on the blade cross-section

Table 3
Hardness of the transverse section of the blade

Point of indentation	1	2	3	4	5	6	7	8	9	10	11
Hardness (HV30)	410	408	400	395	395	396	389	387	406	410	417

from the blade airfoil near the fracture surface and blade root. Fig.2.7 illustrates the micrographs of the material. As to be observed the microstructure has composed of dendritic grains (Fig. 2.7a), which is a characteristic of cast structures. There is a relatively compact scale on the surface of the blade. Although this scale was not continuously built up all over the surface, in some regions there is a noticeably thick scale (Figs.2.7b and c). Underneath the scale, a severe deterioration can be noticed. The severity of this deterioration was to a greater degree in the samples of leading edge, especially on the concave surface. This is in relation with the results of visual examination. Figs. 2.7a and b shows that there are a lot of micro cracks were initiated from the surface. Metallographic examination at higher magnifications carried out by means of scanning electron microscope (SEM). Microprobe analysis was carried out on the scale and subscale regions

(Fig. 9) using an Energy Dispersive X-ray (EDX) analyzer attached to the SEM. The surface scale is comprised of three main components marked with number 1 to 3. In the external region (number 1), the scale composed of relatively unprotective nickel and cobalt oxides. The middle area (number 2) is primarily constituted of protective chromium and aluminum oxides. The internal layer (number 3) is comprised of chromium sulfide and chromium oxide which is the sign of hot corrosion. Furthermore, presence of sulfur at the subscale (number 4) was detected. Also it is observed that the nickel percentage was decreased and the cobalt percentage was increased at subscale which is signifying the depletion of nickel from subscale.

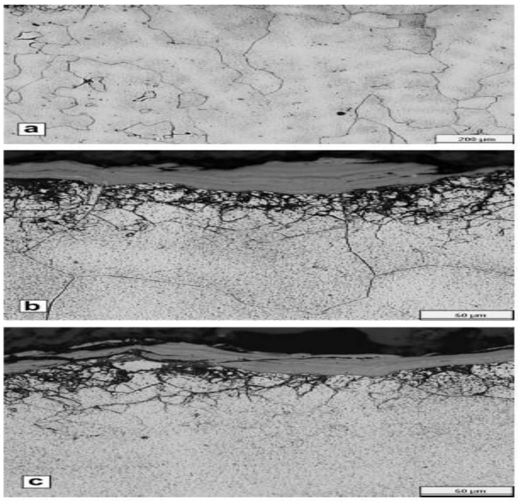

Fig. 2.7. Optical micrograph of the blade material. (a) Dendrite microstructure. (b) Surface scale and subscale deterioration. (c) Same as from another place.

2.6 Analysis of the Fracture Surface

Fracture surface of the failed blade was examined by stereomicroscope and SEM. General View of the fracture surface is shown in Fig. 3.8. Two regions were clear on the surface. The first region which has marked with rectangular is the crack initiation area and the second region which has marked with an ellipse is the crack propagation by fatigue mechanism. Fig. 2.9 has taken from the area inside the rectangular of Fig. 2.8 at higher magnification. As observed in this figure the dendrite morphology is clear on the surface. This morphology demonstrates that the crack path has been interdendritic at initiation area. It can be considered as a sign of hot corrosion. Fig. 2.10 exhibits a high magnification fractograph from the region inside the ellipse in Fig. 2.11 In this area fatigue marks (striations) are evident. It indicates that after the initiation of the crack, propagation has conducted by the fatigue mechanism due to the vibration of the blade. Fig. 2.11 illustrates two fractographs of different magnifications from disconnected regions in the vicinity of fatigue crack propagation. It demonstrates that the crack growth was occurred with different stress levels and frequencies. After crack growth and subsequent reduction in cross-section area, final fracture has occurred in the trailing edge of the blade.

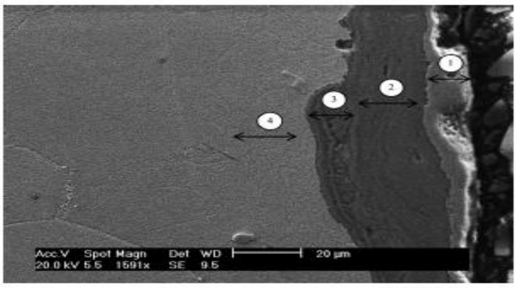

Fig.2.8. Regions of microprobe analysis.

Fig. 2.9 General view of the fracture surface.

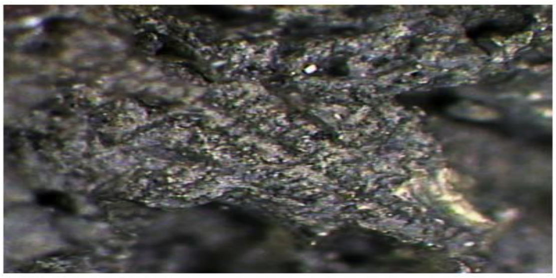

Fig. 2.10 Dendrite morphology in the vicinity of the rectangular in Fig. 2.9. 20x.

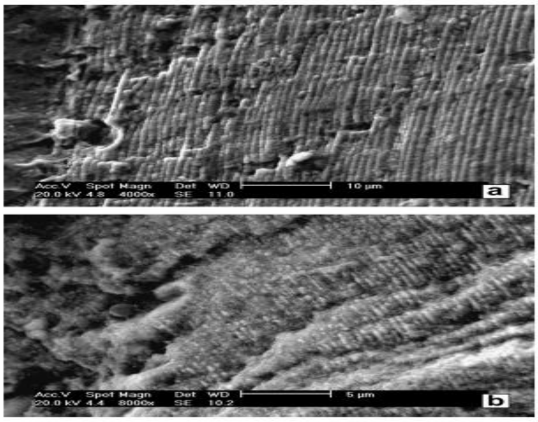

Fig. 2.11. Fatigue striations in the vicinity of the ellipse in Fig. 2.9 from different regions. (a) 4000x. (b) 8000x

3. RESULTS AND DISCUSSION

3.1 Turbine Blade Failure

The main cause of turbine blade failure is high cycle fatigue. Fatigue failure is related to repeated cycling of the load on a structural member. The fatigue life of a structural member i.e. the number of load cycles it can survive is in general determined by the magnitude of the stress cycles. The exact relation between the magnitudes of the stress and the fatigue life depends on the material properties of the structural member. In general higher stresses lead to a shorter fatigue life. For some materials fatigue only occurs if stresses exceed a certain minimum level for other materials there is no minimal stress level. If the stresses that are present on the turbine blade during operation and the material properties of the turbine blade are known then an estimation of the fatigue life of the turbine blade can be made.

3.2 Metallurgical Properties of the Blades

Table 2 shows chemical composition of the blade material compared with the AMS 4928Q standard limits of Ti6Al4V alloy. It confirms that the composition of the fractured blade is similar to the standard Ti6Al4V alloy. The microstructures of the blade root and airfoil in the 2nd failure occurrence are presented in Figs. 3.1 a and b, respectively. As it can be seen, it is predominantly consisted of equaled a-grains, lamellar transformed a plates, and fine intergranular b phases. The portion of lamellar structure in the airfoil is higher than the root. It should be noticed that this microstructure is common in Ti-alloy compressor and fan blades, with equaled portion providing good tensile ductility and hence good resistance to crack initiation, while the lamellar portion is responsible for increasing resistance to crack propagation. Similar microstructures were found for the blades fractured in other failure occurrences of Hesa gas turbines.

Table 2
Chemical composition of the blading alloy

Sample	Standard		Compressor blade	
	Min	Max	Mean	RSD
Al	5.50	6.75	5.18	1.95
V	3.50	4.50	3.91	1.31
Fe	-	0.30	0.15	17.9
Zr	-	-	<0.10	-
Mn	-	-	<0.10	-
Mo	-	-	<0.50	-
Sn	-	-	<0.50	-
Nb	-	-	<0.50	-
Pd	-	-	0.19	0.74
Ti	Rem		88.16	0.08

Hardness values of the root and airfoil of two failed blades are presented in Table 3. The root and airfoil both had the same hardness. Tensile properties of the samples with different work hours are shown in Table 4, representing no significant difference from the standard values. It can be seen that the mechanical and metallurgical properties of the blade material are in the standard range and no deviation in these properties were detected.

Table 3
Vickers hardness of the blade's root and airfoil in two failures

		Fracture number	
		2nd	3rd
Position	Airfoil	359.3	353.3
	Root	335.8	338.2

Table 4
Mechanical properties of the fractured blades

Sample	AMS 4928Q Standard (min)	1st fracture	2nd fracture	3rd fracture	Mean
YS [MPa]	862	992	961	984	979
UTS [MPa]	931	1085	1093	1025	1067.7
Elongation [%]	10	10	11.8	16	12.6
Reduction of Area [%]	25	26	39.2	33	32.7

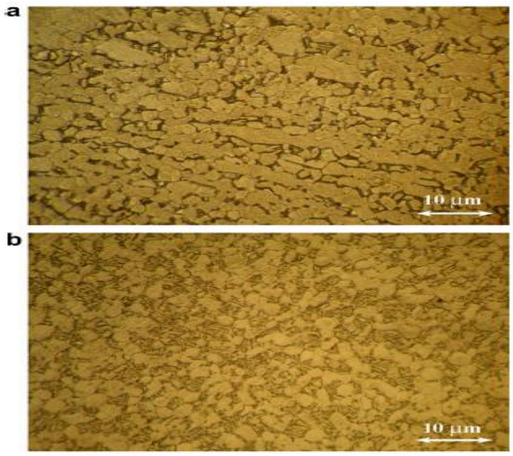

Figs. 3.1 a and b show macro-fractography images of the fracture surfaces of the blade roots failed in the 2^{nd} and the 3rd occurrences

4. CONCLUSIONS

The fretting fatigue mechanism as the main cause of several premature failures of Ti6Al4V alloy compressor blades was characterized. No metallurgical and mechanical deviations were found for the blade material with respect to the standards. Instead, the fretting characteristics were distinguished in the fracture surfaces. The developed 2D numerical model clearly showed that stress concentration was occurred at the corner of EOC in the dovetail region. This directly implies that the cracking was responsible to blade stresses induced in service, and not a product of an isolated defect or anomaly within the component. The high level of stress at the contact surface can be due to the insufficient clearance between the blade root and the disk in the dovetail region. This stress concentration can initiate several cracks which eventually lead to the complete failure of the blade.

The catastrophic failure of the blade has occurred by the following sequence:

1. Formation of the non-protective nickel and cobalt oxides.
2. Formation of the chromium sulfide and depletion of the alloying elements.
3. Degradation of the metal beneath the scale.
4. Progression of the pitting over the concave and convex surfaces of the blade.
5. Deepening of the pits at the leading and trailing edges due to the bending stresses.
6. Development of the inter dendrite corrosion at the leading edge and initiation of the crack.
7. The propagation of crack by the fatigue mechanism because of the vibration of blade in a resonant condition.
8. Reduction of the cross-section area and the final fracture at the trailing edge.

REFERENCES

[1] E. Poursaeidi , M. Aieneravaie (2007**), "Failure analysis of a Second stage blade in a gas turbine engine";** Engineering failure analysis; 15 (2008) pp 1111-1129.

[2] A. Kermanpur (2008), **"Failure analysis of Gas turbine compressor blade";** Engineering failure analysis; 15 (2008) pp 1052-1064.

[3] Z. Mazur (2004) **"Failure analysis of gas turbine blade made of Inconal 738LC alloy";** Engineering failure analysis; 12 (2005) 474-486.

[4] Jung-Chel Chang (2003) **"Failure analysis of gas turbine buckets";** Engineering failure analysis; 10 (2003) pp 559-567**.**

[5] N. J. Lourenco (2007), **"Fatigue failure of a compressor blade";** Engineering failure analysis; 15 (2008) pp 1150-1154.